Published in final edited form as:
Dev Biol. 2010 February 1; 338(1): 1–14. doi:10.1016/j.ydbio.2009.10.029.

Dhrs3a Regulates Retinoic Acid Biosynthesis through a Feedback Inhibition Mechanism

L. Feng[1,2], **R.E. Hernandez**[1,2,3], **J.S. Waxman**[4], **D. Yelon**[4], and **C.B. Moens**[1,2]

[1] Division of Basic Science and HHMI, Fred Hutchinson Cancer Research Center, B2-152, 1100 Fairview Ave. N, Seattle WA 98109

[2] Molecular and Cellular Biology Graduate Program, University of Washington, Seattle.

[3] Medical Scientist Training Program, University of Washington

[4] Developmental Genetics Program and Department of Cell Biology, Kimmel Center for Biology and Medicine at the Skirball Institute of Biomolecular Medicine, New York University School of Medicine, New York, NY, 10016, USA

Abstract

Retinoic acid (RA) is an important developmental signaling molecule responsible for the patterning of multiple vertebrate tissues. RA is also a potent teratogen, causing multi-organ birth defects in humans. Endogenous RA levels must therefore be tightly controlled in the developing embryo. We used a microarray approach to identify genes that function as negative feedback regulators of retinoic acid signaling. We screened for genes expressed in early somite-stage embryos that respond oppositely to treatment with RA versus RA antagonists, and validated them by RNA *in situ* hybridization. Focusing on genes known to be involved in RA metabolism, we determined that *dhrs3a*, which encodes a member of the short-chain dehydrogenase/reductase protein family, is both RA dependent and strongly RA inducible. Dhrs3a is known to catalyze the reduction of the RA precursor all-trans retinaldehyde to vitamin A, however a developmental function has not been demonstrated. Using morpholino knock down and mRNA over-expression, we demonstrate that Dhrs3a is required to limit RA levels in the embryo, primarily within the central nervous system. Dhrs3a is thus an RA-induced feedback inhibitor of RA biosynthesis. We conclude that retinaldehyde availability is an important level at which RA biosynthesis is regulated in vertebrate embryos.

Keywords

zebrafish; retinoic acid; dhrs3; retinoid metabolism; negative feedback; nervous system development; hindbrain; rdh10

Introduction

Retinoic acid, generated from dietary vitamin A, is essential for a wide array of developmental processes, broadly controlling the patterning and differentiation of tissues

derived from all three germ layers (Duester 2008). RA functions in the development of the nervous system, including brain, eye and neural crest (Reviewed by Maden, 2006; Maden, 2007; White and Schilling, 2008); of the heart (Keegan et al., 2005; Waxman et al., 2008), the kidney (Wingert et al., 2007), the gut (Wang et al., 2006), the pancreas (Stafford et al., 2004), and the germ line (Luo et al., 2006).

In many developmental contexts, RA works as a fate determinant, directing structures adjacent to its source to follow different developmental trajectories depending on the level of RA they receive (Maden, 2007). For example, in zebrafish the anterior lateral plate mesoderm (APLM) region will give rise to the heart, the blood precursor cells and the future pectoral fin, and the relative sizes of each precursor pool depends on RA levels (Schoenebeck and Yelon., 2007; Waxman et al., 2008). Thus it is critical for normal development that the distribution of RA in embryonic tissues be tightly controlled (Niederreither and Dolle, 2008).

All-trans RA, the developmentally active form of RA (hereafter referred to simply as RA) is metabolized from all-trans retinaldehyde, which is the direct derivative of Vitamin A (Fig. 1). RA activates gene expression in target tissues through the activation of DNA-bound nuclear receptors. In early vertebrate development, the source of RA is the anterior paraxial mesoderm where its biosynthetic enzyme, Aldh1a2 is expressed, and *aldh1a2* mutants have multi-system defects due to the absence of RA (Grandel et al., 2002;Mic et al. 2002;Niederreither et al., 2002). While localization of *aldh1a2* expression is a key level at which the tissue distribution of RA is controlled, multiple other enzymes in the RA biosynthetic and degradation pathways function to tightly regulate RA bioavailability. Best characterized among these are the Cyp26 enzymes, which eliminate RA in a strictly patterned manner in the hindbrain to set the boundaries of Hox gene expression (Sirbu et al., 2005;Hernandez et al., 2007). On the biosynthetic side, Rdh10, member of the short-chain dehydrogenase/reductase (SDR) family, which oxidizes retinol to retinaldehyde, is expressed in defined domains that overlap with sites of *aldh1a2* expression, and RDH10 mutant mice exhibit a spectrum of RA-deficient phenotypes (Cammas et al., 2007;Sandell et al., 2007;Strate et al., 2009)(Fig. 1). In addition, the non-uniform distribution of RA receptors in the embryo further refines domains of RA responsiveness (Waxman and Yelon, 2007).

All the major developmental signaling pathways are subject to negative feedback inhibition (Barolo and Posakony, 2002; Kitano, 2004). This is also a feature of biosynthetic pathways, where the presence of a downstream metabolite suppresses the expression or function of an upstream enzyme. Feedback regulation is known to occur at multiple levels in the RA signaling pathway (Fig. 1). At the biosynthetic level, *aldh1a2* transcription is inhibited directly by activated RA receptors (Dobbs-McAuliffe et al., 2004; Elizondo et al., 2000). Rdh10 expression is also suppressed by endogenous RA in Xenopus embryos (Strate et al., 2009). Conversely, mesodermal expression of the degrading enzyme Cyp26a1 is strongly RA-inducible (Dobbs-McAuliffe et al., 2004; Hu et al., 2008). At the signaling level, even the relatively simple RA signal transduction cascade is under negative feedback regulation. For example, the RA receptor corepressor RIP140 is RA-induced, and silencing its induction enhances RA responsiveness (White et al., 2003). While over 500 other genes have been reported to be directly or indirectly regulated by RA in some context (Arima et al., 2005; Bouillet et al., 1995; Freemantle et al., 2002; Ishibashi et al., 2003), the potential functions of these genes in feedback regulation of RA signaling in the embryo has not been investigated directly.

Here we used a microarray-based screen in the zebrafish to identify RA target genes that function in early developmental patterning events. To identify endogenous RA targets, either

positive or negative, we validated genes that were inversely affected by treatment with RA and the pan-RAR antagonist AGN193109 compared to untreated controls. Many of these genes have been previously reported to be regulated by RA, such as *cyp26a1*, hox genes and hox co-factors (Freemantle et al., 2002; Hernandez et al., 2004; Kudoh et al., 2002; Maves and Kimmel, 2005; Simeone et al., 1995; Wada et al., 2006; Wang et al., 2007); nuclear hormone receptors *rxrga*, *nr2f1a* and *nr2f6b* (Qiu et al., 1996; Tallafuss et al., 2006), *hnf1b* (*tcf2*) (Hernandez et al., 2004), and *nrip1b* (*rip140*) (Heim et al., 2007). We also identified a number of genes not previously known to be RA-responsive.

One validated RA target encodes a short-chain dehydrogenase/reductase, Dhrs3a (previously called retSDR1), which is related to Rdh10 (Pares et al., 2008). Whereas Rdh10 oxidizes all-trans retinol (vitamin A) to all-trans retinal (Wu et al., 2002) *in vivo*, Dhrs3 has retinaldehyde reductase activity on retinoids, principally reducing all-trans retinal to all-trans retinol (Haeseleer et al., 1998). Zebrafish *dhrs3a* is expressed in the paraxial and lateral plate mesoderm in an RA-dependent manner. Using morpholino knockdown and mRNA over-expression, we demonstrate that Dhrs3a functions to limit RA signaling in the central nervous system. We conclude that the RA-inducible expression of Dhrs3a, which functions to remove the immediate precursor of RA, is a new level of RA feedback control active in the early embryo.

Materials and methods

Fish strains

Our wild-type line for morpholino and mRNA injection experiments is *AB. Other fish lines used in this paper are *cyp26a1*$^{rw716/rw716}$*/giraffe* mutants (Emoto et al., 2005), *aldh1a2*$^{i26/i26}$*/neckless* mutants (Begemann et al., 2001), and the transgenic *Tg(12XRARE-ef1a:gfp)sk71* line which functions as a RA-responsive reporter (detailed characterization will be reported elsewhere: Waxman and Yelon, manuscript submitted). All fish lines were maintained under standard conditions at 28.5°C and were staged by hours post fertilization (hpf) as described (Kimmel et al., 1995).

Embryo pharmacological treatments

Embryos were collected from group natural crosses and treated as described (Hernandez et al., 2004). Embryos used for the microarray analysis were treated with 0.33 M atRA, 10 M AGN 193109, 1 μM AGN 193109 or 2% DMSO, all diluted 1:50 from stock solutions in DMSO. Embryos used for *in situ* hybridization validation were treated with 0.33μM atRA, 10 μM DEAB or 0.1% DMSO, all diluted 1:1000 from stock solutions. The effectiveness of drug treatments for microarray analysis was confirmed by *in situ* hybridization with *egr2b* (*krox20), mafba (val), hoxd4a* and *erm*, whose hindbrain expression patterns change in stereotyped ways in response to RA addition or depletion (Hernandez et al., 2004).

RNA isolation, Microarray hybridization and data analysis

RNA was extracted using the Qiagen RNeasy RNA Isolation Kit (Qiagen, CA, USA). All sample labeling and hybridizations, as well as chip processing and imaging were performed with strict adherence to Affymetrix's standardized protocols in the FHCRC microarray core facility. A single cycle of target synthesis and labeling was used for all samples. Array normalization was performed using GCRMA (Wu et. al. 2004). Significant changes in expression level were identified using CyberT (Baldi and Long, 2001), a Bayesian t-statistic derived for microarray analysis. Significance was determined by ranking the Bayesian p-values and using a false discovery rate methodology (FDR) to account for multiple testing (Reiner et al., 2003). A FDR of 5% was used for the analysis. The complete microarray data set was deposited in NCBI GEO (Accession: GSM409450, GSM409449, GSM409448,

GSM409447, GSM409446, GSM409445, GSM409444, GSM409443, GSM409442, GSM409441, GSM409440, GSM409439, GSM409438, GSM409437, GSM409436 and GSM409435)

Sequence analysis, cloning and constructs

Each EST sequence was used to search the zebrafish genome in UCSC database (http://genome.ucsc.edu/) and Zfin (http://zfin.org/) by pair-wise blast analysis to confirm the nomination. Templates for probe synthesis were produced from previously published constructs or public ESTs as summarized in Table1. ESTs were selected as probe template only if their alignments to the Affymetrix target sequence for a given probe are higher than 97%.

Immunohistochemistry

Antibody staining of whole-mounted embryos with RMO-44 was performed essentially as described (Waskiewicz et al., 2001).

Morpholinos

Three antisense morpholinos were designed to block Dhrs3a function: a translational blocker MO1 5′cccaacaccttcatctccatcatgg3′, and two splice blockers MO3 5′agatgcagtattcttacctttttccc3′ and MO3+ 5′aagattcattggtttatatacctga3′ (Suppl. Fig 1A). To determine the efficiency of MO1, we made a *dhrs3a*-RFP fusion construct by cloning a fragment of the 5' UTR and 5' coding sequence including the MO target sequence into pCS2-mRFP (Suppl. Fig 1B). The resulting plasmid was linearized with NotI and mRNA was prepared for injection with the SP6 mMessage mMachine kit (Ambion, TX, USA). Embryos injected with 250 pg fusion protein mRNA show strong RFP expression, while co-injection of 5 ng MO1 blocks the fusion RFP expression (Suppl. Fig 1C, 1D). Live images were taken using a Leica fluorescent dissection Microscope with the same settings.

We used RT-PCR to determine the efficacy of Dhrs3a MO3 set, which is targeted to the exon-2ntron-2 splice junction of the pre-mRNA. Primer pair F- 5'-AAGCAAGGAGCGAGAAAGGTG-3', R- 5'-TCGTGGTCCAGAACTGTCCAAG-3' was used to check the efficiency of these MOs (Suppl. Fig1A). MO3 alone creates a 21bp insertion due to the use of a cryptic splice donor in intron 2 (not shown). When combined with MO3+, which targets this splice donor, the two MOs produce a 60bp deletion due to the use of another cryptic splice donor in exon 2 (Fig. S1E). The resulting 20 aa deletion is expected to disrupt the helix/β-sheet/helix sandwich structure shared by all short-chain dehydrogenase/reductase (Pares et al., 2008 and according to the 3D structure of DHRS1 [PDB 2QQ5]). In all of our assays for Dhrs3a activity, the MO3 set was less effective than MO1, possibly because of some limited function of the deleted version of the protein. Since both MO1 and MO3 set caused a degree of toxicity to injected embryos (Suppl. Fig 1F), we co-injected a *tp53 (p53)* MO that suppresses cell death at 5ng/emb as described (Robu et al., 2007) and reduced the toxicity of MOs (Suppl. Fig 1F). The 5ng/emb *tp53 MO* was also used in control injections.

dhrs3a mRNA injection

mRNA was synthesized from whole length cDNA clone (GenBank: BC078383.1) [Openbiosystem, IL, USA], by using the mMessenger Machine kit (Ambion, TX, USA) as described (Hernandez et al., 2004). mRNA 300pg/emb was injected (Suppl. Fig 1F).

RNA *in situ* hybridizations and genotyping

Two-color RNA *in situ* hybridizations were performed, essentially as described (Prince et al., 1998), except that NBT/BCIP (Roche, IN, USA) and INT/BCIP stocks (Roche, IN, USA) premixed stock were used as the Alkaline Phosphatase substrate. Double fluorescent RNA *in situ* hybridization was performed as described (Julich et al., 2005), with some modification (Ma et al., 2008). Embryos were de-yolked and flat-mounted for photo-microscopy using a Zeiss Axioplan II microscope. After photographing, individual embryos were un-mounted and genotyped for the *cyp26a1* or *aldh1a2* mutations as described (Begemann et al., 2001; Emoto et al., 2005).

RNA reverse transcription (RT) and Quantitative real-time PCR

An aliquot of each RNA extract was used for spectrophotometry to determine RNA quality and concentration. RNA with a 260/280 ratio among 1.95–2.2 was considered good quality and was used for Reverse Transcription. RT with heat-denaturation of RNA was carried out using the RETRO script kit (Ambion, TX, USA). Random decamers were used according to the manufacturer's instructions. Tests were taken to make sure there is no genomic DNA contamination.

Quantitative PCR was carried out on an ABI Prism 7900 HT sequence detection system (Applied Biosystems, CA, USA) with SYBR green fluorescent label. Samples contained 1× SYBR green master mix (Applied Biosystems, CA, USA), 3 pmol of each primer and 0.2 μl RT reaction for a final volume of 10 μl. Each sample was run in triplicate in optically clear 96-well plates (Applied Biosystems, CA, USA) and PCR was performed twice on each sample. Cycling parameters were as follows: 50°C × 2 min, 95°C × 10 min, then 40 cycles of the following 95°C × 15 s, 57°C × 50 s and 72°C × 30 s. A dissociation module was performed at the end of the amplification phase in which the temperature rose from 55°C to 95°C with 1°C a step for 30 s to identify a single, specific melting temperature for each amplicon.

Eight housekeeping genes were evaluated from commonly used reference genes and a primer set for *gapdh* was picked for the control amplicon (Supplementary Table 1). All oligonucleotide primers were developed using online Primer3 software (http://frodo.wi.mit.edu/) and further checked by Amplify 3X software and were synthesized by Operon (AL, USA). Primer sequences are shown in supplementary table 1. Primer sets were tested for specificity using standard RT-PCR and zebrafish embryo cDNA as template to verify production of a single band of the predicted size.

Data Analysis was performed as described (McCurley and Callard, 2008). Student's t-tests were used to test the null hypothesis that there was no significant difference between treatment samples and the control sample. One-way analysis of variance (ANOVA) was used to compare gene expression between different treatment groups. Where significant differences were identified, the Newman-Kuels test was used to determine which groups differ from each other.

Confocal Microscope imaging of *Tg(12XRARE-ef1a:gfp)sk71* transgenic line

Heterozygous *Tg(12XRARE-ef1a:gfp)sk71* transgenic fish were crossed to non-transgenic wild-type fish and injected with control or *dhrs3* MOs at the 1-cell stage. Transgene-expressing embryos were staged at 46 hours based on the emergence of expression in the retina, which is unaffected in MO-injected embryos. GFP-expressing embryos were mounted in 0.6% agarose at 48hpf and imaged with a Zeiss Pascal inverted confocal microscope. Z-stacks included the entire dorsoventral extent of CNS GFP expression plus

one section on either side. Fluorescent intensity and area were determined using Volocity software (Improvision, PerkinElmer, MA. USA).

Results

Microarray identification of RA-responsive genes in the embryo

To identify RA-responsive genes, we treated embryos with 0.33μM all-trans (at-RA; henceforth referred to as simply RA) starting at 6.5 hpf. This concentration is sufficient to consistently posteriorize zebrafish embryos based on the loss of *mafba (val)* expression from rhombomere 5 and 6 and the expansion of *hoxd4a* expression to the anterior end of the embryo (Fig. 2). To identify the subset of RA-responsive genes that normally require RA for their expression or whose expression is normally suppressed by RA in the early embryo, we treated embryos with 10μM of the pan-RAR antagonist AGN193109 from 5.25 hpf (Agarwal et al., 1996), which phenocopies a zebrafish RA production mutant *aldh1a2*$^{i26/i26}$ (Linville et al., 2004). We also used a lower concentration (1 μM) of AGN193109 to partially block RA signaling. Microarray analysis and *in situ* validation were performed on whole 11 hpf treated embryos and controls.

We compared expression levels of each EST between control (DMSO treated) embryos and embryos with RA treatment, and between control embryos and embryos with either 10μM or 1μM AGN193109 treatment. Significant changes in expression level were identified using CyberT (Baldi and Long, 2001), a Bayesian t-statistic derived for microarray analysis. Significance was determined by ranking the Bayesian p-values and using a false discovery rate methodology to account for multiple testing (Reiner et al., 2003). A false discovery rate of 5% was used for the analysis.

We wanted to identify endogenous direct or indirect RA targets that are expressed in the early somite stage embryo. RA-dependent genes are expected to be found at increased levels in RA treated embryos and at decreased levels in AGN193109 treated embryos. We identified 321 ESTs whose expression was significantly increased in RA-treated embryos. Of these 321 ESTs, only 29 genes exhibited decreased expression with AGN193109 treatment (Table 1). This large difference between the number of RA-induced and antagonist-suppressed genes was observed in a similar microarray screen in Xenopus (Arima et al., 2005) and reflects the fact that many RA-inducible genes are not expressed at early somite stages when we performed our microarray experiment, so they could not be suppressed by antagonist. In contrast, almost all of the genes whose expression was significantly decreased in AGN193109 were also up-regulated in RA. We also identified 287 ESTs whose expression decreased significantly in response to RA treatment. The most strongly down-regulated are genes that are normally expressed in the mid- and forebrain (e.g. *irx7, otx1, eng2a, mab21l2)*. This is not surprising considering that the concentration of RA used in this experiment normally expands posterior hindbrain markers throughout the brain (Fig. 2). Consistent with this, only a small subset of these ESTs (5/287) were significantly increased in expression as a result of AGN193109 treatment (Table 1). Only two genes were significantly affected in the same direction by both RA and AGN193109 treatment: *cyp26b1* was upregulated by both, and *val/mafB* was down regulated by both.

We focused our validation efforts on the genes that were inversely affected by RA and RA antagonist treatments. Of the 34 genes that were significantly affected in opposite directions by RA and RA antagonist, 18 were previously reported to be controlled by RA either in embryos or in cultured cells. *cyp26a1* (Emoto et al., 2005), *hnf1b* (Hernandez et al., 2004), *tbx1* (Roberts et al., 2005; Zhang et al., 2006), *tshz1* (Wang et al., 2007), *dhrs3a* (Waxman et al., 2008), and several anterior hox genes (Maves and Kimmel, 2005; Morrison et al., 1997; Waxman et al., 2008) are all RA-regulated in zebrafish or Xenopus embryos (Arima

et al., 2005). Additionally, *meis2* (Mercader et al., 2000; Niederreither et al., 2000), *nr2f1*, *nr2f6* (*ear2*) (Jonk et al., 1994) *hoxd11* (Bel-Vialar et al., 2000), *nrip1* (Freemantle et al., 2002) and *hoxa3a* (Mulder et al., 1998) were reported to be RA-induced in mouse embryos or in cultured cells.

RNA *in situ* validation of RA-responsive genes

We chose 21 of these 34 genes (18 coding plus 3 non-coding) to test by RNA *in situ* hybridization in control, RA-treated and antagonist-treated embryos. For RNA *in situ* validation, we used the Aldh1a2 antagonist DEAB, which blocks RA synthesis, in place of AGN193109. Control experiments demonstrated that the effects of DEAB and AGN193109 are indistinguishable. We chose primarily genes that were not previously identified as RA-responsive, or genes whose RA responsiveness had not previously been demonstrated in embryos by RNA in situ hybridization. 17 out of 21 genes were successfully validated as being affected in both RA- and antagonist-treated embryos (Table 1, Fig. 3, Fig. 4 and Supplementary Fig. 2). The four genes that failed to validate gave low, ubiquitous signal in both treated and untreated embryos. In addition, we validated a further 23 novel RA targets that were significantly affected by RA and conversely affected by AGN193109 in three of four biological replicates, but where the effect of AGN193109 was below our significance cut-off (Table 1, Fig. 3, Fig. 4 and Suppl. Fig. 2).

Many of the validated hits showed RA-dependent activation or repression in the anterior trunk region. This is the region where RA levels are normally highest due to *aldh1a2* expression in the anterior paraxial mesoderm (see Fig. 6F for *aldh1a2* expression). Fig. 3 and Fig. S1 show genes whose expression is RA-dependent and RA-inducible, while Fig. 4 shows the smaller number of validated genes whose expression is normally RA-suppressed. Many genes including *rxrga, wnt11r, nrip1b, nr2f6b (*Fig. 3A-D*), hoxb5a and ap1gbp1* (Fig. S2A, B*)* are normally expressed in this region in ectoderm and/or lateral mesoderm. In each case, this expression is reduced or eliminated in inhibitor-treated embryos and expanded anteriorly in RA-treated embryos. In contrast, RA-dependent expression of *pgp* and cullin3 in the anterior somitic and adaxial mesoderm is expanded posteriorly within that compartment in the presence of RA (Fig. 3E and S2L). Other genes/ESTs, (e.g. spsb4, znf503, znf703, tsc22d3, dact2, cyp24a1l, odz3, meis2.1, tiparp and a non-coding RNA located 3′ of the nova1 gene) are more broadly expressed in untreated embryos, but their expression in the anterior trunk region is specifically RA-dependent (Fig. 3F, S2C-K). Other tissue-specific gene expression was also RA-dependent and RA-inducible, such as *meis2.1* expression in the ventral mesoderm (Fig. S2I), *hnf1g and claudinC expression* in the pronephric mesoderm (Fig. 3G, S2O), *crabp2a* expression in the anterior notochord (Fig. S2M) and a gene fragment with homology to human MYT1, which is expressed in early-differentiating neurons in the anterior spinal cord in an RA-dependent manner (Fig. 3H). This requirement for RA for gene expression in multiple tissue types is consistent with the multi-organ defects in RA-deficient animals.

We also identified genes that are normally repressed by RA. Negative effects on gene expression by RA are likely to be indirect since RAR transcriptional activity is generally increased, not suppressed, in the presence of RA. *tbx1* expression in pharyngeal endoderm is repressed by RA (Fig. 4A)(Roberts et al., 2005;Zhang et al., 2006). We also discovered that *her3*, a hairy-related gene that functions to suppress neurogenesis in the inter-proneural domain of the spinal cord (Bae et al., 2005) is normally repressed by RA in the anterior spinal cord where the earliest neuronal differentiation occurs (Fig. 4B). Similarly, *hey2/ gridlock* expression is upregulated in the anterior spinal cord of DEAB-treated embryos and suppressed by RA treatment (Fig. 4C). Expression of genes such as *hey2* and *cdc42ep4* that are normally expressed in cephalic mesoderm are expanded posteriorly in DEAB-treated embryos and eliminated in RA-treated embryos, suggesting that RA normally functions to

establish their posterior limit in the ventral mesoderm (Fig. 4C,D). Genes normally restricted to hindbrain rhombomeres anterior to r5, such as *dusp2* and *cyp26b1* are similarly expanded in DEAB-treated embryos, consistent with their being indirectly regulated by RA-dependent hindbrain patterning events (Hernandez et al., 2007)(Fig. 4E,S2N). Cyp26b1 but not dusp2 is induced in cranial mesoderm by RA as described previously (White and Schilling, 2008).

Previous work demonstrated a role for the *Rdh10* gene in RA metabolism (Sandell et al., 2007). *Rdh10* encodes a retinol oxidase that metabolizes retinol into retinaldehyde, the immediate precursor of RA (Wu et al., 2002). Strate et al. (2009) found that *Rdh10* expression is suppressed by RA and increased in RA-depleted Xenopus embryos, suggesting a negative feedback loop in which the presence of sufficient levels of RA would shut off further retinaldehyde, and thus RA, production. The zebrafish genome contains two *rdh10* genes, *rdh10a* and *10b*. We examined expression of both genes and found that *rdh10a* is expressed in the paraxial mesoderm in early somite stage embryos. Neither *rdh10a* or *10b* were represented on the microarray we used in our experiments, so to determine whether this negative feedback loop was active during zebrafish development we examined *rdh10a* expression in RA-treated and RA-depleted embryos at the 3 somite stage. We found that RA-depleted embryos had significantly increased *rdh10a* expression, while RA-treated embryos had reduced *rdh10a* expression (Fig. 4F). Rdh10a expression was also affected in *aldh1a2* and *cyp26a1* mutants, but only very weakly (data not shown). Together with our findings below, this suggests that the reversible reaction that converts retinol to retinaldehyde is an important level at which RA biosynthesis is controlled.

Dhrs3a is an RA-dependent retinal dehydrogenase

One of the RA-responsive genes with most significant changes on our microarray was *dhrs3a. dhrs3a* expression was induced 15-fold by RA and repressed 11-fold by AGN193109 (Table 1). Similar RA-responsiveness for dhrs3a was observed in a separate microarray experiment in zebrafish (Waxman et al. 2008). We validated this by *in situ* hybridization in RA- and antagonist- treated embryos as well as in mutant embryos *aldh1a2*$^{i26/i26}$*/neckless* (which have reduced RA levels) and *cyp26a1*$^{rw716/rw716}$*/giraffe* (which have increased endogenous RA levels)(Fig. 5). At early somite stages, dhrs3 is expressed in the lateral plate mesoderm posterior to the heart fields, in tissue that is fated to contribute to the anterior (pectoral) limbs (Waxman et al., 2008), as well as more medially, in mesoderm immediately anterior to the somites. This expression is entirely RA-dependent, since it is lost in embryos where RA is depleted chemically (Fig. 5B) or genetically (Fig. 5E). The expression is also sensitive to endogenous RA levels, since it is expanded in *cyp26a1* mutants (Fig. 5F). *dhrs3a* expression is expanded throughout the embryo after treatment with RA (Fig. 5C).

dhrs3a expression is first detected in the mesoderm at 6.5 hpf, expanding to include the paraxial and lateral mesoderm by the end of gastrulation (Fig. 6A-C). This early expression overlaps fully with that of *aldh1a2* (Fig. 6G). However, during early somite stages *dhrs3a* and *aldh1a2* expression diverges, with *dhrs3a* expression becoming restricted to mesoderm lateral and anterior to the *aldh1a2*-expressing anterior somites (Fig. 6D-I). A closely related duplicate gene, *dhrs3b*, has non-overlapping expression in the yolk syncytial layer during gastrulation and later in the spinal cord and tailbud (Thisse and Thisse, 2004).

Dhrs3a regulates RA signaling

Dhrs3 has been identified in multiple microarray experiments as a strongly RA-inducible gene, however its function has not been assessed *in vivo* (Arima et al., 2005; Cerignoli et al., 2002; Waxman et al., 2008). *dhrs3* encodes a short-chain dehydrogenase/reductase that catalyses the reduction of all-trans retinal to all-trans retinol, lowering the bioavailability of

RA precursor (Haeseleer et al., 1998; Jornvall, 2008). Since we found that *dhrs3a* is expressed in an RA-dependent manner, we hypothesized that Dhrs3a may function as a feedback inhibitor of RA biosynthesis, by eliminating the immediate RA precursor. We thus tested Dhrs3a function with antisense morpholinos and mRNA over-expression (see materials and methods and suppl. Fig. 1).

If Dhrs3a functions to control RA biosynthesis by reducing retinaldehyde bioavailability, we predicted that the expression of known RA target genes would be increased in Dhrs3a morphants and decreased in embryos over-expressing *dhrs3a*. *cyp26a1* expression is a sensitive read-out of RA levels in the zebrafish (Abu-Abed et al., 2001; Loudig et al., 2005; Reijntjes et al., 2005). In early somite stage embryos (12 hpf), *cyp26a1* is expressed weakly in a domain that overlaps with *dhrs3a* expression in mesoderm anterior and lateral to the RA-producing anterior somites (Fig. 7A). We found that the level of *cyp26a1* expression is increased and this domain is expanded in early somite-stage embryos injected with two different *dhrs3a* morpholinos (Fig. 7D,E). Quantitative PCR for *cyp26a1* expression in control and MO-injected embryos confirmed this result: *cyp26a1* expression in *dhrs3a* MO-injected samples is at least 2-fold higher than both the uninjected or control MO-injected samples, when normalized with *gapdh* (Fig. 7G). In contrast, when *dhrs3a* is over-expressed by mRNA injection at the 1-cell stage, *cyp26a1* expression is reduced at 12hpf (Fig. 7F, compare to 7C).

A more direct way to visualize RA signaling is through the expression of a reporter driven by a RA-response element (RARE). We used a RA-responsive transgenic line *Tg(12XRARE-ef1a:gfp)sk71* (Waxman and Yelon Manuscript submitted). RA-responsive GFP is expressed in the anterior spinal cord up to a sharp anterior limit at the rhombomere 6/7 boundary (Fig. 7I). This expression is entirely RA-dependent, as it is eliminated in DEAB-treated embryos and induced throughout the CNS in RA-treated embryos (data not shown). We found that injection of *dhrs3a* MOs results in an increase both in the length of the RARE-eGFP expression domain and in the overall level of GFP expression at 48 hpf (Fig. 7K, L compare to Fig.7J and 7I). In contrast, when *dhrs3a* is over-expressed by mRNA injection, both the RARE-eGFP expression domain and the overall of GFP expression are reduced at 48 hpf (Fig.7H, compare to 7I). Quantitative analysis of RARE-eGFP expression in control, mRNA-injected and MO-injected embryos further confirmed this result (Fig.7M). The increase in both *cyp26a1* expression and in RARE-eGFP reporter expression in *dhrs3a*-depleted embryos is consistent with a model in which Dhrs3a functions to reduce the bioavailability of RA precursor.

Dhrs3a controls nervous system organization—The region of the embryo immediately anterior to the anterior-most somites experiences highest RA signaling in the early somite stage zebrafish embryo, as reflected by RARE-GFP reporter expression and by multiple *in situ*-validated RA targets identified in our microarray screen, all of which exhibit RA-responsiveness in this domain. The length of this domain is determined by RA levels, as reflected by its shortening in *aldh1a2*$^{i26/i26}$*/neckless* mutants (Begemann et al., 2001) and its lengthening in *cyp26a1*$^{rw716/rw716}$*/giraffe* mutants (Emoto et al., 2005). Focusing on the central nervous system, we defined the distance from the second somite (defined morphologically and by the anterior limit of *pax2a* expression in pronephric mesoderm) up to the r6/7 boundary as the “high RA” domain, which corresponds to the domain of *hoxd4a* (Fig. 8A) and *rxrga* expression (Fig. 2A), both of which are RA targets (Maves and Kimmel, 2005; Waxman and Yelon, 2007). We compared this distance, which is normally approximately 250μm, between *aldh1a2*$^{i26/i26}$*/neckless* mutants, *cyp26a1*$^{rw716/rw716}$*/giraffe* mutants, *dhrs3a* MO-injected embryos and their control siblings (Fig. 8A-C). The length of this region is increased by 26% in cyp26a1/gir mutants and decreased by over 60% in aldh1a2/nls mutants (data not shown). Compared to this, the effects of *dhrs3a* knockdown

were mild. Nevertheless, we observed a subtle (~6%) but statistically significant increase in the length of the "high RA" domain in Dhrs3a morphants (dotted arrows in Fig. 8A-C). A similar increase in the distance from the second somite to r3 was also observed (solid arrows in Fig. 8A-C). This phenotype is consistent with a role for Dhrs3a in regulating RA levels in the embryo.

Neuroanatomically, the "high RA" region includes anterior-most spinal cord and hindbrain rhombomere 7/8. No clear boundary separates r7 from r8, however there are neuroanatomical differences: in zebrafish r7 contains CaD and CaV interneurons as well as the nucleus of the glossopharyngeal nerve, while r8 contains the large vagus motor nucleus (Chandrasekhar et al., 1997; Kimmel, 1982; Kimmel et al., 1982). Additionally, a set of contralaterally projecting T-reticular interneurons differentiate dorsally in r7 and r8 (Kimmel et al., 1985) and can be detected with the RMO44 antibody (Waskiewicz et al., 2001). In *cyp26a1*/gir mutants, anterior spinal cord fates are shifted anteriorly and the vagal region is correspondingly reduced (Emoto et al., 2005) while in *aldh1a2*/nls mutants, more anterior hindbrain fates are shifted posteriorly, also resulting in a reduced vagal region (Begemann et al., 2004). Similarly, we found that the number of RMO44-positive T-interneurons was reduced in both *aldh1a2*$^{i26/i26}$*/neckless* and *cyp26a1*$^{rw716/rw716}$*/giraffe* mutants (Fig. 9 and data not shown). We found that the length of the vagus motor nucleus is quite variable even in control embryos, and we did not observe consistent effects on its length in Dhrs3a morphants. However the number of T-interneurons is affected. Control embryos contain an average of 4.7 RMO44-positive T-interneurons while *dhrs3a* MO embryos contain an average of 4 such neurons. Moreover, whereas only 5% of control embryos contained 3 or fewer T-interneurons, between 25 and 35% of *dhrs3a* MO embryos did (Fig. 9F).

Interactions with other RA-regulating genes

If Dhrs3a normally functions as a feedback inhibitor of RA biosynthesis, we predicted that depleting it would enhance the phenotype of *cyp26a1*$^{rw716/rw716}$*/giraffe* mutants in which RA levels are also increased due to reduced degradation. On the other hand, we did not expect *dhrs3a* knockdown to suppress the phenotype of *aldh1a2*/nls mutants, since Aldh1a2 is epistatic to Dhrs3a in the RA biosynthesis pathway (Fig. 1). We injected embryos from *cyp26a1*$^{+/rw716}$ or *aldh1a2*$^{+/i26}$ incrosses with *dhrs3a* MOs, and sorted the resulting embryos based on the known morphological *aldh1a2* and *cyp26a1* mutant phenotypes (Begemann et al., 2001;Emoto et al., 2005) and examined them for changes in hindbrain patterning and neuroanatomical phenotypes caused by *dhrs3a* depletion.

cyp26a1 mutants have a subtle hindbrain patterning phenotype whereby r4 is elongated and r7 is reduced in length (Fig. 8E). Dhrs3a morphants have no detectable hindbrain patterning defect aside from the subtle lengthening of the posterior hindbrain described above (Fig. 8B, C). However *cyp26a1*$^{rw716/rw716}$ embryos injected with Dhrs3a MOs exhibited an enhanced phenotype in which the entire hindbrain was shortened and r3 was strongly reduced or absent (Fig. 8F, G). This is similar to the phenotype of *cyp26a1* mutants in which RA degradation is further inhibited by depletion of the partially redundant Cyp26c1 enzyme (Hernandez et al., 2007). We also observed an enhancement of the posterior hindbrain neuroanatomical defects described above. *cyp26a1* mutants have a reduced number of T-reticular interneurons compared to controls (Fig. 9C, E) and this number is further reduced by Dhrs3a depletion (Fig. 9E). Together, these additive phenotypes are consistent with a model in which Dhrs3a and Cyp26a1 function to deplete RA levels in the zebrafish embryo through independent pathways (Fig. 1). As predicted, we saw no suppression of the *aldh1a2* mutant phenotype as a result of Dhrs3a depletion (data not shown).

Discussion

In this study, we have used microarray analysis to identify genes that are directly or indirectly regulated by RA in the early somite stage zebrafish embryo. Our approach, which was to compare both RA-treated and antagonist treated expression profiles to untreated controls and to focus on genes that behave oppositely in the two treatments, allowed us to identify the small subset of RA-inducible and RA-suppressible genes on our microarray that are bona fide RA targets in the early somite stage embryo. Previous screens for RA-regulated genes in cultured cells, *Ciona* or *Xenopus* embryos compared RA-treated to controls or RA-treated directly to antagonist-treated embryos and thereby identified hundreds of potential RA targets (Bouillet et al., 1995, Freemantle et al., 2002, Ishibashi et al., 2003, 2005, Arima et al., 2005). These included orthologs of some of the genes we validated as endogenous RA targets in our zebrafish microarray such as *nrip1*(RIP140), DHRS3, CYP26A1, TCF2, HOX and MEIS genes, however without the corresponding RA depletion expression profile the *in vivo* significance of many of these hits has remained unclear.

We identified RA target genes expressed in all three germ layers. The majority of validated hits are expressed in an RA-dependent manner in the anterior trunk, while a smaller subset of validated hits are normally repressed by RA in this region. RA is synthesized by Aldh1a2 in the anterior somitic mesoderm, and has its strongest effects on neural patterning and organogenesis in this region. For example, RA specifies the position of the pectoral fin, pancreas and proximal segments of the pronephros at the level of the anterior-most somites, and limits the posterior extent of the heart fields (Begemann et al., 2001; Grandel et al., 2002; Keegan et al. 2005; Stafford and Prince, 2002; Waxman et al., 2008). Consistent with this, we saw the most dramatic effects on gene expression in RA-treated and antagonist-treated embryos in this region. It remains to be determined whether the RA targets we have identified mediate the effects of RA on these developmental processes.

In the neurectoderm, we identified genes like *wnt11r, rxrga*, and *nr2f6b*, which exhibit RA-dependent expression throughout the anterior spinal cord, up to the rhombomere 6/7 boundary which is a common anterior limit of RA-dependent gene expression. The anterior spinal cord is the earliest site of neuronal differentiation within the CNS, but how this localization of neurogenesis along the anterior-posterior axis is achieved is not fully understood. We found that markers of early differentiating neurons such as *myt1* exhibited RA-dependent expression in the anterior spinal cord. Other neurogenic genes such as *neurogenin1* and *deltaB* behaved similarly on our microarray (not shown). Recent work has demonstrated that early neuronal differentiation in the mouse spinal cord depends on the direct positive regulation of neurogenic genes by RA (Ribes et al., 2008), while work in the zebrafish has shown that neurogenesis is suppressed in the inter-proneural domains of the spinal cord by the hairy-related gene *her3* (Bae et al., 2005). Our finding that *her3* is itself normally suppressed by RA in the anterior spinal cord adds a new level at which RA controls neurogenesis, by simultaneously activating neurogenic genes and suppressing expression of a suppressor of neurogenesis.

Microarray analysis identifies regulators of RA metabolism

A number of the genes identified in our microarray screen and validated by RNA *in situ* hybridization encode proteins that regulate retinoid metabolism (e.g. the RA degrading enzymes *cyp26a1* and *cyp26b1*) or retinoic acid receptor function (e.g. *nrip1*/rip140, *nr2f6* and *nr2f1*). The identification of these genes as RA targets underscores the multiple levels at which RA signaling is regulated by feedback control mechanisms in the embryo (Beland and Lohnes, 2005; Dobbs-McAuliffe et al., 2004; Hernandez et al., 2007; White et al., 2003). We found that the short-chain dehydrogenase/reductase family member *dhrs3a* was among

the most strongly RA-regulated gene, being 15-fold up-regulated in RA and 11-fold down-regulated in AGN193109, a result we confirmed by *in situ* hybridization in RA-treated and RA-depleted embryos and mutants. Whether RA functions directly or indirectly in Dhrs3a regulation remains to be determined, however we note that there are multiple canonical retinoic acid response elements near the *dhrs3a* genes of multiple vertebrate species (see also Waxman and Yelon, 2008).

Dhrs3a is a member of a large family of short chain dehydrogenase/reductases, many of which have been demonstrated to be active on retinoids (Pares et al., 2008). Dhrs3 has been demonstrated to preferentially catalyze the reduction of retinaldehyde to retinol *in vitro* (Haeseleer et al., 1998). We hypothesized that RA-dependent activation of *dhrs3a* could result in the removal of retinaldehyde, thereby acting as a negative feedback regulator of RA production. Indeed, we found that in *dhrs3a* knock-down embryos, RA levels are increased as judged by increases in RA-dependent *cyp26a1* expression and RARE-GFP reporter expression in the spinal cord. Depletion of Dhrs3a enhanced the posteriorized hindbrain phenotype of *cyp26a1* mutants, in which RA levels are increased due to decreased degradation. We note that depletion of Dhrs3a did not rescue the RA-depleted phenotype of *aldh1a2* mutants, consistent with Aldh1a2 being epistatic to Dhrs3a in the RA biosynthesis pathway (Fig. 1).

Dhrs3a is related to mammalian Rdh10 (Dalfo et al., 2007), which oxidizes retinol to retinaldehyde, thereby controlling the availability of RA precursor (Wu et al., 2002). Rdh10 mutant mice have a RA-deficiency phenotype similar to (but milder than) that of Aldh1a2 mutants, and this phenotype can be suppressed by supplementing maternal RA (Sandell et al., 2007). We observed that zebrafish *rdh10a* is expressed in the RA-producing paraxial mesoderm, and that this expression is suppressed by endogenous RA and is increased in the absence of RA, as shown previously in *Xenopus* (Fig. 4F; Strate et al., 2009). This sets up a negative feedback loop whereby RA inhibits further synthesis of its own precursor (Fig. 1). In contrast, Dhrs3, which requires NADPH rather than NAD as a cofactor, preferentially catalyzes the reverse reaction, reducing retinaldehyde to retinol in vitro (Haeseleer et al., 1998), and its expression in anterior trunk mesoderm is strongly induced by endogenous RA. This sets up an alternative negative feedback loop whereby RA synthesis is inhibited by the active elimination of its precursor (Fig. 1). Taken together, our work and that of Sandell et al. and Strate et al. suggest that two key enzymes, one functioning as a retinaldehyde reductase and the other functioning in retinol oxidation, play complementary roles in controlling the availability of the RA precursor retinaldehyde. In this model, in the presence of RA, Dhrs3a-dependent retinaldehyde reduction is activated and Rdh10-dependent retinol oxidation is suppressed. This is predicted to result in a rapid drop in retinaldehyde levels. In the absence of RA, retinaldehyde is able to accumulate. This feedback regulation of retinaldehyde levels functions in parallel to the more direct negative feedback regulation on RA itself by suppression of *aldh1a2* and activation of *cyp26* exrpession (Fig. 1). The relative importance of these negative feedback mechanisms is likely to vary in different organisms and stages of development where the composition of maternally provided retinoids is different. Furthermore, the various feedback mechanisms may be differentially employed in different cell types. In this regard it is notable that in the early somite stage embryo the two enzymes that work positively in the biosynthesis of RA, Rdh10 and Aldh1a2, are expressed within the anterior somitic mesoderm while the two enzymes that serve to remove retinaldehyde and RA, respectively, Dhrs3a and Cyp26, are primarily expressed in the ventral and lateral mesoderm surrounding the anterior somites. Understanding the spatial and temporal requirements for these various feedback mechanisms will require higher resolution characterization of *rdh10a* and *dhrs3a* expression and of the effects of their knock-down in specific RA-dependent developmental processes.

Supplementary Material

Refer to Web version on PubMed Central for supplementary material.

Acknowledgments

We wish to thank Jeff Delrow in the FHCRC microarray facility for help with designing, performing and analyzing the microarray experiments. Jen-Wei Huang performed some of the in situ validation experiments. We also thank Sean Rhodes and Yuri Rabena for expert zebrafish care. The members of the Moens lab provided helpful comments on this manuscript. This work was supported by NIH grant HD37909 to CBM; NIH grant F32HL083591 and K99HL091126 to JSW and NIH grant R01 HL069594 to DY. CBM is an Investigator with the Howard Hughes Medical Institute.

References

Abu-Abed S, Dolle P, Metzger D, Beckett B, Chambon P, Petkovich M. The retinoic acid-metabolizing enzyme, CYP26A1, is essential for normal hindbrain patterning, vertebral identity, and development of posterior structures. Genes Dev 2001;15:226–40. [PubMed: 11157778]

Agarwal C, Chandraratna RA, Johnson AT, Rorke EA, Eckert RL. AGN193109 is a highly effective antagonist of retinoid action in human ectocervical epithelial cells. J Biol Chem 1996;271:12209–12. [PubMed: 8647816]

Arima K, Shiotsugu J, Niu R, Khandpur R, Martinez M, Shin Y, Koide T, Cho KW, Kitayama A, Ueno N, Chandraratna RA, Blumberg B. Global analysis of RAR-responsive genes in the Xenopus neurula using cDNA microarrays. Dev Dyn 2005;232:414–31. [PubMed: 15614783]

Bae YK, Shimizu T, Hibi M. Patterning of proneuronal and inter-proneuronal domains by hairy- and enhancer of split-related genes in zebrafish neuroectoderm. Development 2005;132:1375–85. [PubMed: 15716337]

Baldi P, Long AD. A Bayesian framework for the analysis of microarray expression data: regularized t -test and statistical inferences of gene changes. Bioinformatics 2001;17:509–19. [PubMed: 11395427]

Barolo S, Posakony JW. Three habits of highly effective signaling pathways: principles of transcriptional control by developmental cell signaling. Genes Dev 2002;16:1167–81. [PubMed: 12023297]

Begemann G, Marx M, Mebus K, Meyer A, Bastmeyer M. Beyond the neckless phenotype: influence of reduced retinoic acid signaling on motor neuron development in the zebrafish hindbrain. Dev Biol 2004;271:119–29. [PubMed: 15196955]

Begemann G, Schilling TF, Rauch GJ, Geisler R, Ingham PW. The zebrafish neckless mutation reveals a requirement for raldh2 in mesodermal signals that pattern the hindbrain. Development 2001;128:3081–94. [PubMed: 11688558]

Bel-Vialar S, Core N, Terranova R, Goudot V, Boned A, Djabali M. Altered retinoic acid sensitivity and temporal expression of Hox genes in polycomb-M33-deficient mice. Dev Biol 2000;224:238–49. [PubMed: 10926763]

Beland M, Lohnes D. Chicken ovalbumin upstream promoter-transcription factor members repress retinoic acid-induced Cdx1 expression. J Biol Chem 2005;280:13858–62. [PubMed: 15677473]

Bouillet P, Oulad-Abdelghani M, Vicaire S, Garnier JM, Schuhbaur B, Dolle P, Chambon P. Efficient cloning of cDNAs of retinoic acid-responsive genes in P19 embryonal carcinoma cells and characterization of a novel mouse gene, Stra1 (mouse LERK-2/Eplg2). Dev Biol 1995;170:420–33. [PubMed: 7649373]

Cammas L, Romand R, Fraulob V, Mura C, Dolle P. Expression of the murine retinol dehydrogenase 10 (Rdh10) gene correlates with many sites of retinoid signalling during embryogenesis and organ differentiation. Dev Dyn 2007;236:2899–908. [PubMed: 17849458]

Cerignoli F, Guo X, Cardinali B, Rinaldi C, Casaletto J, Frati L, Screpanti I, Gudas LJ, Gulino A, Thiele CJ, Giannini G. retSDR1, a short-chain retinol dehydrogenase/reductase, is retinoic acid-inducible and frequently deleted in human neuroblastoma cell lines. Cancer Res 2002;62:1196–204. [PubMed: 11861404]

Chandrasekhar A, Moens CB, Warren JT Jr. Kimmel CB, Kuwada JY. Development of branchiomotor neurons in zebrafish. Development 1997;124:2633–44. [PubMed: 9217005]

Dalfo D, Marques N, Albalat R. Analysis of the NADH-dependent retinaldehyde reductase activity of amphioxus retinol dehydrogenase enzymes enhances our understanding of the evolution of the retinol dehydrogenase family. FEBS J 2007;274:3739–52. [PubMed: 17608724]

Dobbs-McAuliffe B, Zhao Q, Linney E. Feedback mechanisms regulate retinoic acid production and degradation in the zebrafish embryo. Mech Dev 2004;121:339–50. [PubMed: 15110044]

Duester G. Retinoic acid synthesis and signaling during early organogenesis. Cell 2008;134:921–31. [PubMed: 18805086]

Elizondo G, Corchero J, Sterneck E, Gonzalez FJ. Feedback inhibition of the retinaldehyde dehydrogenase gene ALDH1 by retinoic acid through retinoic acid receptor alpha and CCAAT/enhancer-binding protein beta. J Biol Chem 2000;275:39747–53. [PubMed: 10995752]

Emoto Y, Wada H, Okamoto H, Kudo A, Imai Y. Retinoic acid-metabolizing enzyme Cyp26a1 is essential for determining territories of hindbrain and spinal cord in zebrafish. Dev Biol 2005;278:415–27. [PubMed: 15680360]

Freemantle SJ, Kerley JS, Olsen SL, Gross RH, Spinella MJ. Developmentally-related candidate retinoic acid target genes regulated early during neuronal differentiation of human embryonal carcinoma. Oncogene 2002;21:2880–9. [PubMed: 11973648]

Grandel H, Lun K, Rauch GJ, Rhinn M, Piotrowski T, Houart C, Sordino P, Kuchler AM, Schulte-Merker S, Geisler R, Holder N, Wilson SW, Brand M. Retinoic acid signalling in the zebrafish embryo is necessary during pre-segmentation stages to pattern the anterior-posterior axis of the CNS and to induce a pectoral fin bud. Development 2002;129:2851–65. [PubMed: 12050134]

Haeseleer F, Huang J, Lebioda L, Saari JC, Palczewski K. Molecular characterization of a novel short-chain dehydrogenase/reductase that reduces all-trans-retinal. J Biol Chem 1998;273:21790–9. [PubMed: 9705317]

Heim KC, White KA, Deng D, Tomlinson CR, Moore JH, Freemantle SJ, Spinella MJ. Selective repression of retinoic acid target genes by RIP140 during induced tumor cell differentiation of pluripotent human embryonal carcinoma cells. Mol Cancer 2007;6:57. [PubMed: 17880687]

Hernandez RE, Putzke AP, Myers JP, Margaretha L, Moens CB. Cyp26 enzymes generate the retinoic acid response pattern necessary for hindbrain development. Development 2007;134:177–87. [PubMed: 17164423]

Hernandez RE, Rikhof HA, Bachmann R, Moens CB. vhnf1 integrates global RA patterning and local FGF signals to direct posterior hindbrain development in zebrafish. Development 2004;131:4511–20. [PubMed: 15342476]

Hu P, Tian M, Bao J, Xing G, Gu X, Gao X, Linney E, Zhao Q. Retinoid regulation of the zebrafish cyp26a1 promoter. Dev Dyn 2008;237:3798–808. [PubMed: 19035346]

Ishibashi T, Nakazawa M, Ono H, Satoh N, Gojobori T, Fujiwara S. Microarray analysis of embryonic retinoic acid target genes in the ascidian Ciona intestinalis. Dev Growth Differ 2003;45:249–59. [PubMed: 12828686]

Jonk LJ, de Jonge ME, Pals CE, Wissink S, Vervaart JM, Schoorlemmer J, Kruijer W. Cloning and expression during development of three murine members of the COUP family of nuclear orphan receptors. Mech Dev 1994;47:81–97. [PubMed: 7947324]

Jornvall H. Medium- and short-chain dehydrogenase/reductase gene and protein families : MDR and SDR gene and protein superfamilies. Cell Mol Life Sci 2008;65:3873–8. [PubMed: 19011752]

Julich D, Hwee Lim C, Round J, Nicolaije C, Schroeder J, Davies A, Geisler R, Lewis J, Jiang YJ, Holley SA. beamter/deltaC and the role of Notch ligands in the zebrafish somite segmentation, hindbrain neurogenesis and hypochord differentiation. Dev Biol 2005;286:391–404. [PubMed: 16125692]

Keegan BR, Feldman JL, Begemann G, Ingham PW, Yelon D. Retinoic acid signaling restricts the cardiac progenitor pool. Science 2005;307:247–9. [PubMed: 15653502]

Kitano H. Biological robustness. Nat Rev Genet 2004;5:826–37. [PubMed: 15520792]

Kimmel CB. Reticulospinal and vestibulospinal neurons in the young larva of a teleost fish, Brachydanio rerio. Prog Brain Res 1982;57:1–23. [PubMed: 7156394]

Kimmel CB, Ballard WW, Kimmel SR, Ullmann B, Schilling TF. Stages of embryonic development of the zebrafish. Dev Dyn 1995;203:253–310. [PubMed: 8589427]

Kimmel CB, Metcalfe WK, Schabtach E. T reticular interneurons: a class of serially repeating cells in the zebrafish hindbrain. J Comp Neurol 1985;233:365–76. [PubMed: 3980775]

Kimmel CB, Powell SL, Metcalfe WK. Brain neurons which project to the spinal cord in young larvae of the zebrafish. J Comp Neurol 1982;205:112–27. [PubMed: 7076887]

Kudoh T, Wilson SW, Dawid IB. Distinct roles for Fgf, Wnt and retinoic acid in posteriorizing the neural ectoderm. Development 2002;129:4335–46. [PubMed: 12183385]

Linville A, Gumusaneli E, Chandraratna RA, Schilling TF. Independent roles for retinoic acid in segmentation and neuronal differentiation in the zebrafish hindbrain. Dev Biol 2004;270:186–99. [PubMed: 15136149]

Loudig O, Maclean GA, Dore NL, Luu L, Petkovich M. Transcriptional co-operativity between distant retinoic acid response elements in regulation of Cyp26A1 inducibility. Biochem J 2005;392:241–8. [PubMed: 16053444]

Luo T, Sakai Y, Wagner E, Drager UC. Retinoids, eye development, and maturation of visual function. J Neurobiol 2006;66:677–86. [PubMed: 16688765]

Ma EY, Rubel EW, Raible DW. Notch signaling regulates the extent of hair cell regeneration in the zebrafish lateral line. J Neurosci 2008;28:2261–73. [PubMed: 18305259]

Maden M. Retinoids and spinal cord development. J Neurobiol 2006;66:726–38. [PubMed: 16688770]

Maden M. Retinoic acid in the development, regeneration and maintenance of the nervous system. Nat Rev Neurosci 2007;8:755–65. [PubMed: 17882253]

Maves L, Kimmel CB. Dynamic and sequential patterning of the zebrafish posterior hindbrain by retinoic acid. Dev Biol 2005;285:593–605. [PubMed: 16102743]

McCurley AT, Callard GV. Characterization of housekeeping genes in zebrafish: male-female differences and effects of tissue type, developmental stage and chemical treatment. BMC Mol Biol 2008;9:102. [PubMed: 19014500]

Mercader N, Leonardo E, Piedra ME, Martinez AC, Ros MA, Torres M. Opposing RA and FGF signals control proximodistal vertebrate limb development through regulation of Meis genes. Development 2000;127:3961–70. [PubMed: 10952894]

Mic FA, Haselbeck RJ, Cuenca AE, Duester G. Novel retinoic acid generating activities in the neural tube and heart identified by conditional rescue of Raldh2 null mutant mice. Development 2002;129:2271–2282. [PubMed: 11959834]

Morrison A, Ariza-McNaughton L, Gould A, Featherstone M, Krumlauf R. HOXD4 and regulation of the group 4 paralog genes. Development 1997;124:3135–46. [PubMed: 9272954]

Mulder GB, Manley N, Maggio-Price L. Retinoic acid-induced thymic abnormalities in the mouse are associated with altered pharyngeal morphology, thymocyte maturation defects, and altered expression of Hoxa3 and Pax1. Teratology 1998;58:263–75. [PubMed: 9894676]

Niederreither K, Dolle P. Retinoic acid in development: towards an integrated view. Nat Rev Genet 2008;9:541–53. [PubMed: 18542081]

Niederreither K, Vermot J, Fraulob V, Chambon P, Dolle P. Retinaldehyde dehydrogenase 2 (RALDH2)- independent patterns of retinoic acid synthesis in the mouse embryo. Proc Natl Acad Sci U S A 2002;99:16111–6. [PubMed: 12454286]

Niederreither K, Vermot J, Schuhbaur B, Chambon P, Dolle P. Retinoic acid synthesis and hindbrain patterning in the mouse embryo. Development 2000;127:75–85. [PubMed: 10654602]

Pares X, Farres J, Kedishvili N, Duester G. Medium- and short-chain dehydrogenase/reductase gene and protein families: Medium-chain and short-chain dehydrogenases/reductases in retinoid metabolism. Cell Mol Life Sci 2008;65:3936–49. [PubMed: 19011747]

Prince VE, Moens CB, Kimmel CB, Ho RK. Zebrafish hox genes: expression in the hindbrain region of wild-type and mutants of the segmentation gene, valentino. Development 1998;125:393–406. [PubMed: 9425135]

Qiu Y, Krishnan V, Pereira FA, Tsai SY, Tsai MJ. Chicken ovalbumin upstream promoter-transcription factors and their regulation. J Steroid Biochem Mol Biol 1996;56:81–5. [PubMed: 8603050]

Reijntjes S, Blentic A, Gale E, Maden M. The control of morphogen signalling: regulation of the synthesis and catabolism of retinoic acid in the developing embryo. Dev Biol 2005;285:224–37. [PubMed: 16054125]

Reiner A, Yekutieli D, Benjamini Y. Identifying differentially expressed genes using false discovery rate controlling procedures. Bioinformatics 2003;19:368–75. [PubMed: 12584122]

Ribes V, Stutzmann F, Bianchetti L, Guillemot F, Dolle P, Le Roux I. Combinatorial signalling controls Neurogenin2 expression at the onset of spinal neurogenesis. Dev Biol 2008;321:470–81. [PubMed: 18590718]

Roberts C, Ivins SM, James CT, Scambler PJ. Retinoic acid down-regulates Tbx1 expression in vivo and in vitro. Dev Dyn 2005;232:928–38. [PubMed: 15736167]

Robu ME, Larson JD, Nasevicius A, Beiraghi S, Brenner C, Farber SA, Ekker SC. p53 activation by knockdown technologies. PLoS Genet 2007;3:e78. [PubMed: 17530925]

Sandell LL, Sanderson BW, Moiseyev G, Johnson T, Mushegian A, Young K, Rey JP, Ma JX, Staehling-Hampton K, Trainor PA. RDH10 is essential for synthesis of embryonic retinoic acid and is required for limb, craniofacial, and organ development. Genes Dev 2007;21:1113–24. [PubMed: 17473173]

Schoenebeck JJ, Yelon D. Illuminating cardiac development: Advances in imaging add new dimensions to the utility of zebrafish genetics. Semin Cell Dev Biol 2007;18:27–35. [PubMed: 17241801]

Simeone A, Avantaggiato V, Moroni MC, Mavilio F, Arra C, Cotelli F, Nigro V, Acampora D. Retinoic acid induces stage-specific antero-posterior transformation of rostral central nervous system. Mech Dev 1995;51:83–98. [PubMed: 7669695]

Sirbu IO, Gresh L, Barra J, Duester G. Shifting boundaries of retinoic acid activity control hindbrain segmental gene expression. Development 2005;132:2611–22. [PubMed: 15872003]

Stafford D, Hornbruch A, Mueller PR, Prince VE. A conserved role for retinoid signaling in vertebrate pancreas development. Dev Genes Evol 2004;214:432–41. [PubMed: 15322880]

Stafford D, Prince VE. Retinoic acid signaling is required for a critical early step in zebrafish pancreatic development. Curr Biol 2002;12:1215–20. [PubMed: 12176331]

Strate I, Min TH, Iliev D, Pera EM. Retinol dehydrogenase 10 is a feedback regulator of retinoic acid signalling during axis formation and patterning of the central nervous system. Development 2009;136:461–72. [PubMed: 19141675]

Tallafuss A, Hale LA, Yan YL, Dudley L, Eisen JS, Postlethwait JH. Characterization of retinoid-X receptor genes rxra, rxrba, rxrbb and rxrg during zebrafish development. Gene Expr Patterns 2006;6:556–65. [PubMed: 16448862]

Thisse, B.; Thisse, C. Fast Release Clones: A High Throughput Expression Analysis. ZFIN Direct Data Submission. 2004. http://zfin.org

Wada H, Escriva H, Zhang S, Laudet V. Conserved RARE localization in amphioxus Hox clusters and implications for Hox code evolution in the vertebrate neural crest. Dev Dyn 2006;235:1522–31. [PubMed: 16538655]

Wang H, Lee EM, Sperber SM, Lin S, Ekker M, Long Q. Isolation and expression of zebrafish zinc-finger transcription factor gene tsh1. Gene Expr Patterns 2007;7:318–22. [PubMed: 17035100]

Wang Z, Dolle P, Cardoso WV, Niederreither K. Retinoic acid regulates morphogenesis and patterning of posterior foregut derivatives. Dev Biol 2006;297:433–45. [PubMed: 16806149]

Waskiewicz AJ, Rikhof HA, Hernandez RE, Moens CB. Zebrafish Meis functions to stabilize Pbx proteins and regulate hindbrain patterning. Development 2001;128:4139–51. [PubMed: 11684652]

Waxman JS, Keegan BR, Roberts RW, Poss KD, Yelon D. Hoxb5b acts downstream of retinoic acid signaling in the forelimb field to restrict heart field potential in zebrafish. Dev Cell 2008;15:923–34. [PubMed: 19081079]

Waxman JS, Yelon D. Comparison of the expression patterns of newly identified zebrafish retinoic acid and retinoid X receptors. Dev Dyn 2007;236:587–95. [PubMed: 17195188]

Waxman, JS.; Yelon, D. Zebrafish retinoic acid receptors function as context-dependent transcriptional activators.. In submission

White KA, Yore MM, Warburton SL, Vaseva AV, Rieder E, Freemantle SJ, Spinella MJ. Negative feedback at the level of nuclear receptor coregulation. Self-limitation of retinoid signaling by RIP140. J Biol Chem 2003;278:43889–92. [PubMed: 14506269]

White RJ, Schilling TF. How degrading: Cyp26s in hindbrain development. Dev Dyn 2008;237:2775–90. [PubMed: 18816852]

Wingert RA, Selleck R, Yu J, Song HD, Chen Z, Song A, Zhou Y, Thisse B, Thisse C, McMahon AP, Davidson AJ. The cdx genes and retinoic acid control the positioning and segmentation of the zebrafish pronephros. PLoS Genet 2007;3:1922–38. [PubMed: 17953490]

Wu BX, Chen Y, Fan J, Rohrer B, Crouch RK, Ma JX. Cloning and characterization of a novel all-trans retinol short-chain dehydrogenase/reductase from the RPE. Invest Ophthalmol Vis Sci 2002;43:3365–72. [PubMed: 12407145]

Wu Z, Irizarry RA, Gentleman R, Murillo FM, Spencer F. A Model Based Background Adjustment for Oligonucleotide Expression Arrays. JASA 2004;99:909–917.

Zhang L, Zhong T, Wang Y, Jiang Q, Song H, Gui Y. TBX1, a DiGeorge syndrome candidate gene, is inhibited by retinoic acid. Int J Dev Biol 2006;50:55–61. [PubMed: 16323078]

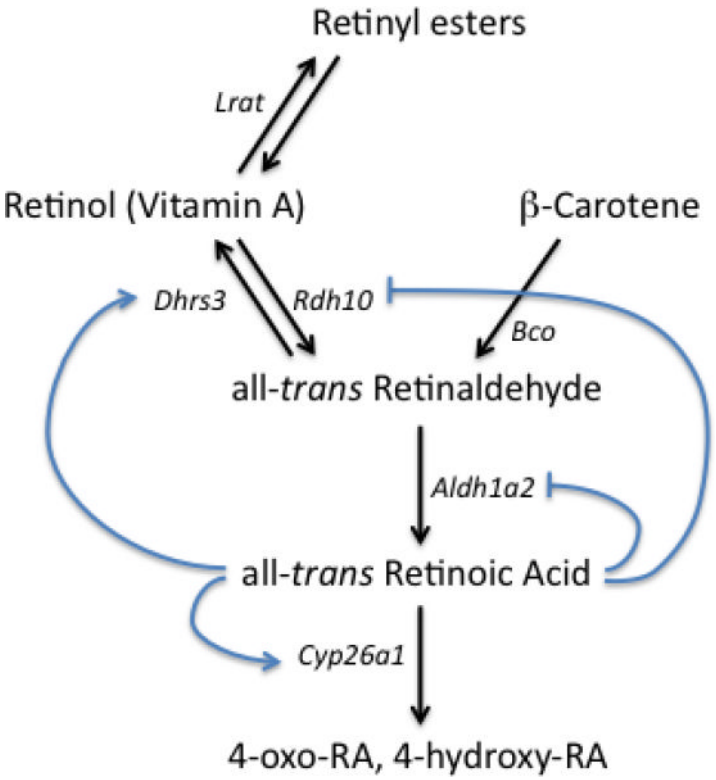

Fig. 1. Schematic of retinoic acid metabolism
Blue arrows indicate levels of feedback control.

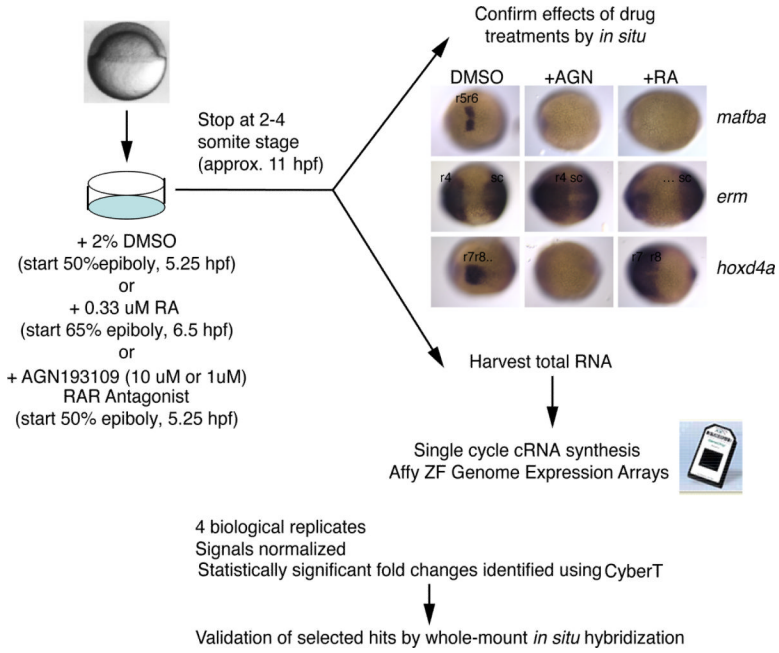

Fig. 2. Strategy for microarray identification of RA-regulated genes

Wild-type embryos were treated with RA, RA signaling antagonist (AGN193109) or DMSO (control) as shown. Treated embryos were collected at the 2-4 somite stage (about 11 hpf). A subset of treated embryos were fixed for *in situ* hybridization with *mafBa, erm, or hoxd4*, to confirm the drug treatment effect, and the remainder was used for RNA harvest. Four separate treatments were performed. After a single cycle of cRNA synthesis, the hybridization was carried out on Affymetrix Zebrafish Genome Expression chips. Selected hits were validated by *in situ* hybridization.

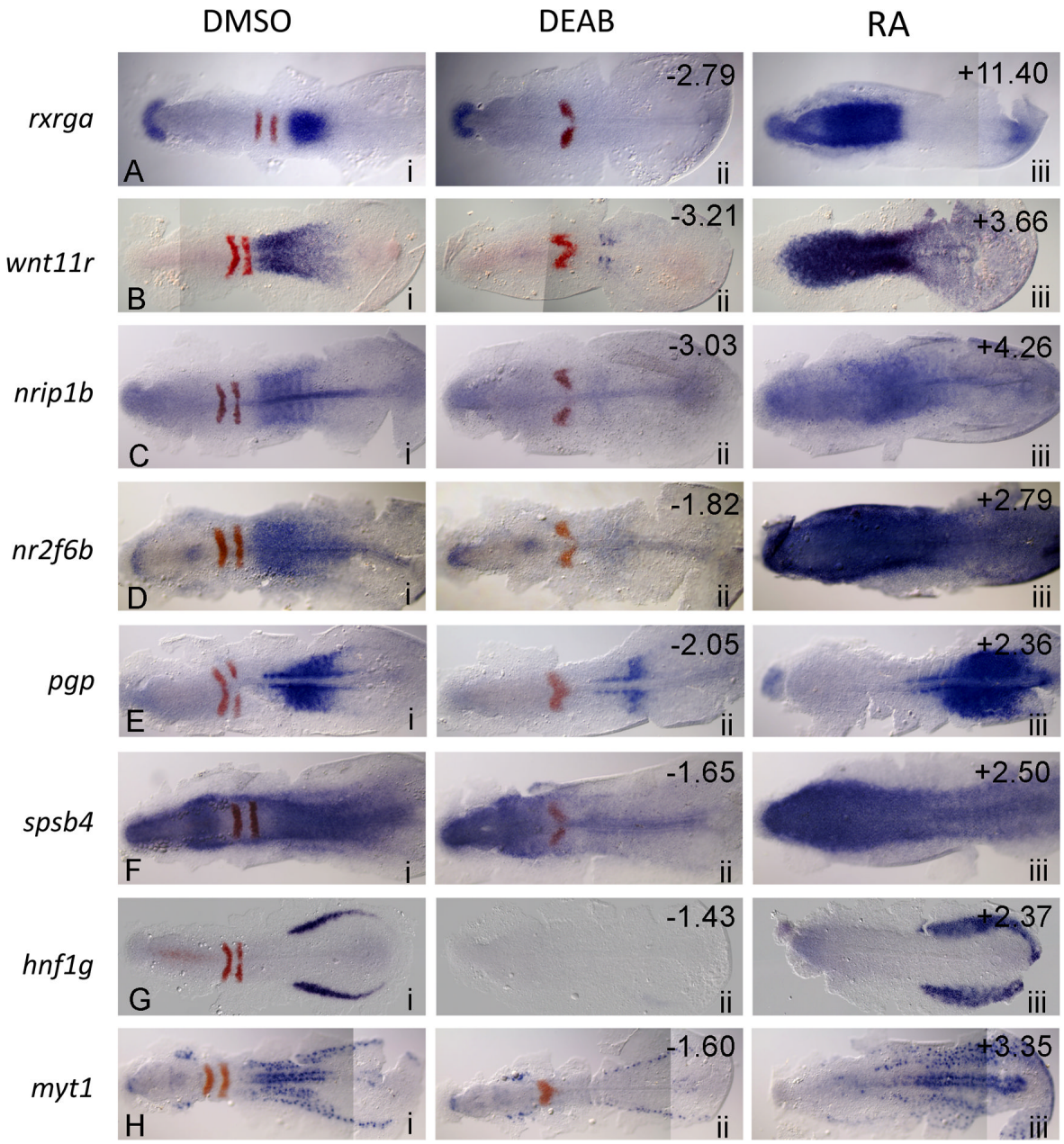

Fig. 3. *In situ* validation of microarray hits whose expression is increased in RA-treated embryos and reduced in antagonist-treated embryos

Dorsal views of 8 selected microarray hits (blue) and *egr2b* (red) in situs at 11hpf. Anterior is to the left in all panels. Column i: control (DMSO) treated; ii: 10 μM DEAB (RA synthesis antagonist) treated; iii: 0.33μM RA-treated. The numbers in the upper right corners refer to the fold-change in expression level identified on the microarray under the corresponding conditions.

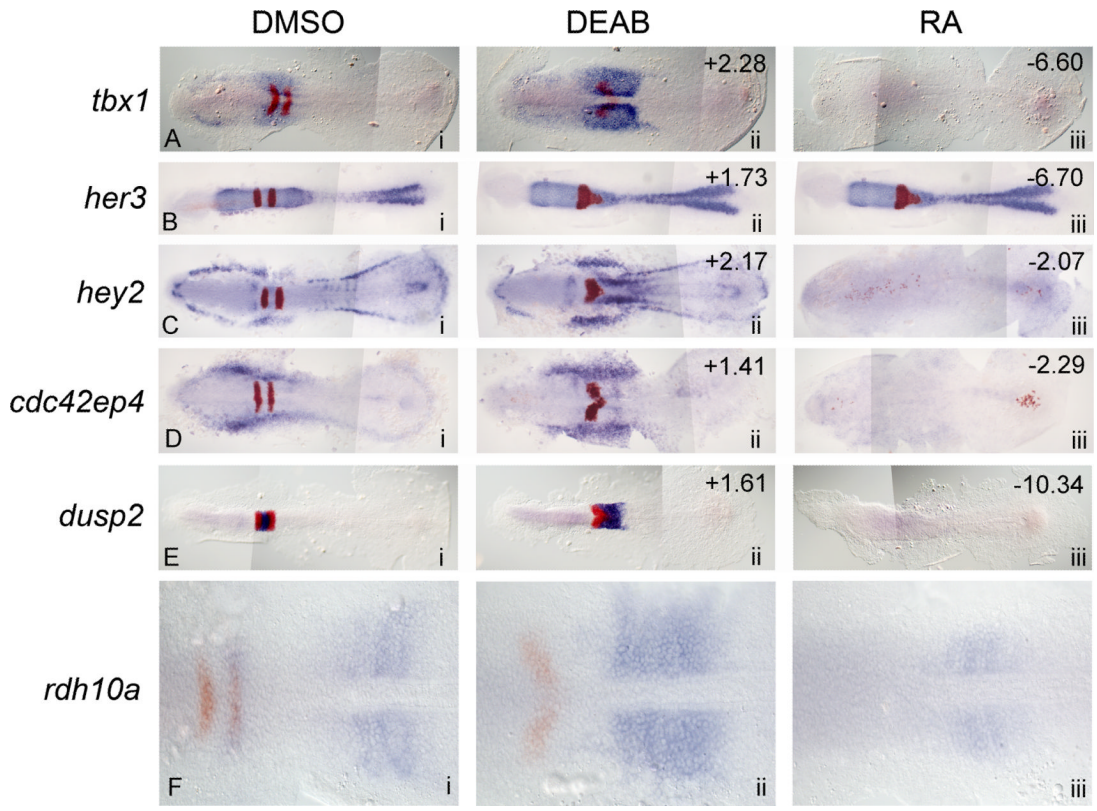

Fig. 4. *In situ* validation of microarray hits whose expression is decreased in RA-treated embryos and increased in antagonist-treated embryos

A-E: Dorsal views of 5 selected microarray hits (blue) and *egr2b* (red) at 11hpf. Anterior is to the left in all panels. Column i: control (DMSO) treated; ii: 10 μM DEAB (RA synthesis antagonist) treated; iii: 0.33μM RA-treated. The numbers in the upper right corners refer to the fold-change in expression level identified on the microarray. F: Although not represented on the microarray, zebrafish *rdh10a* is increased in RA-depleted embryos and suppressed in RA-treated embryos.

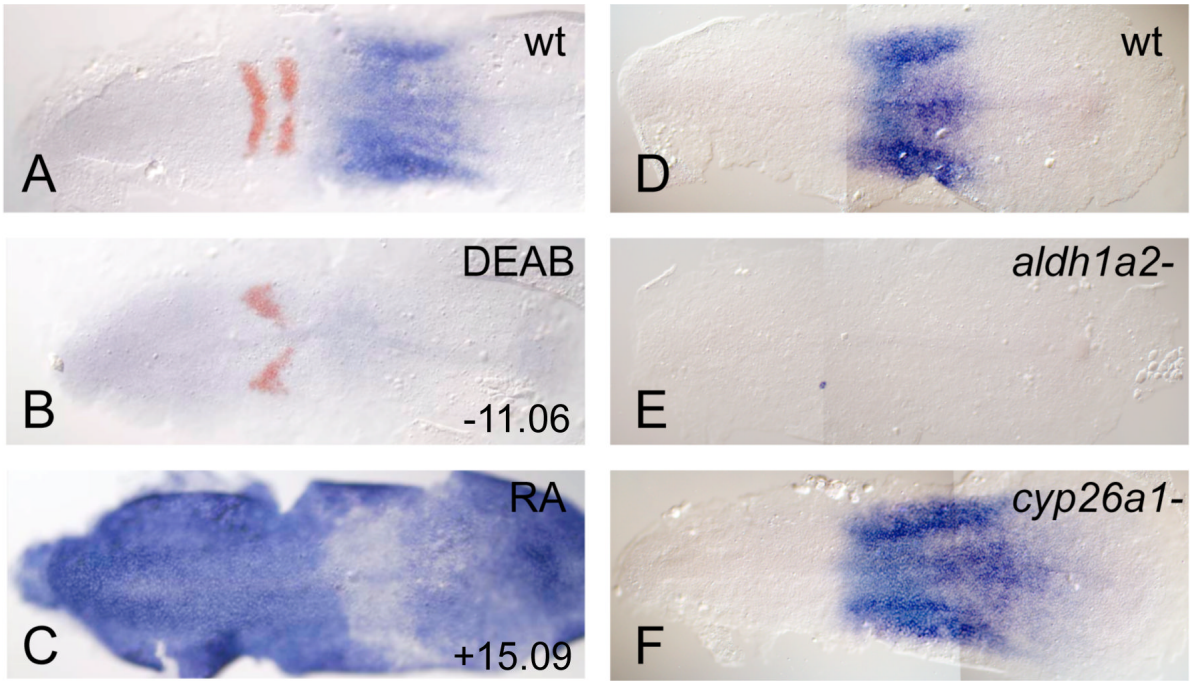

Fig. 5. *dhrs3a* is expressed in an RA-dependent manner

RNA *in situ* hybridization of of *dhrs3a* (blue) and *egr2b* (red in A-C). (A) DMSO-treated; (B) 10 μM DEAB-treated, (C) 0.33μM RA-treated. (D) wild-type untreated, (E) *aldh1a2*$^{i26/i26}$*/neckless* mutant, (F) *cyp26a1*$^{rw716/rw716}$*/giraffe* mutant. Anterior is to the left in all panels.

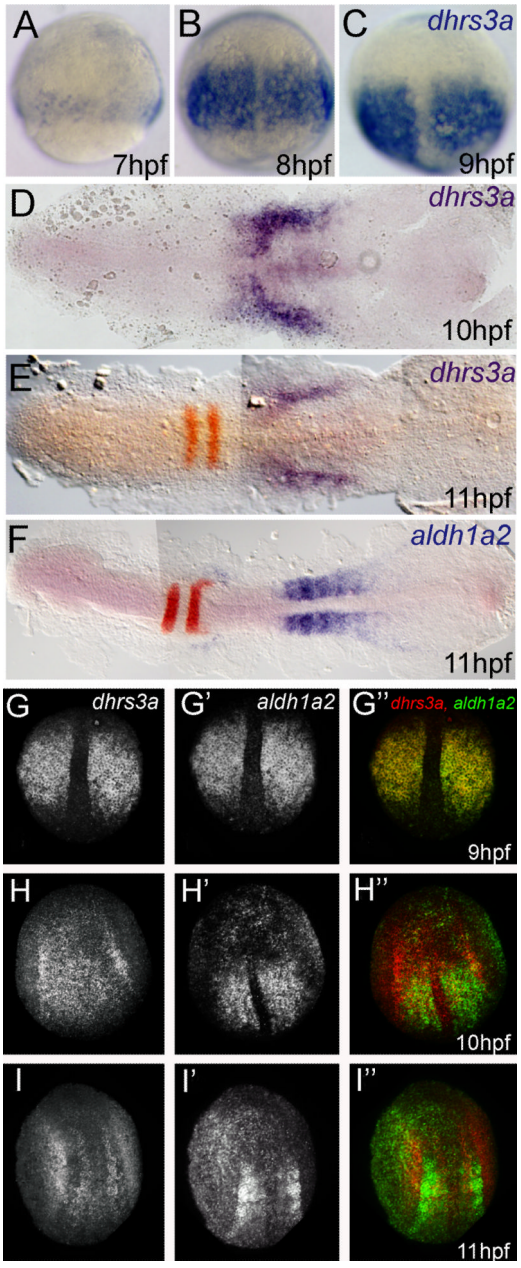

Fig. 6. *dhrs3a* expression is dynamic and correlated with *aldh1a2 expression*

Chromogenic *(A-F)* and fluorescent *(G-I) in situ* hybridization of *dhrs3a* (A-E, G-I), *aldh1a2* (F, G′-I′) and both (G″, H″ and I″). The red color in E- F shows the expression of *egr2b*.

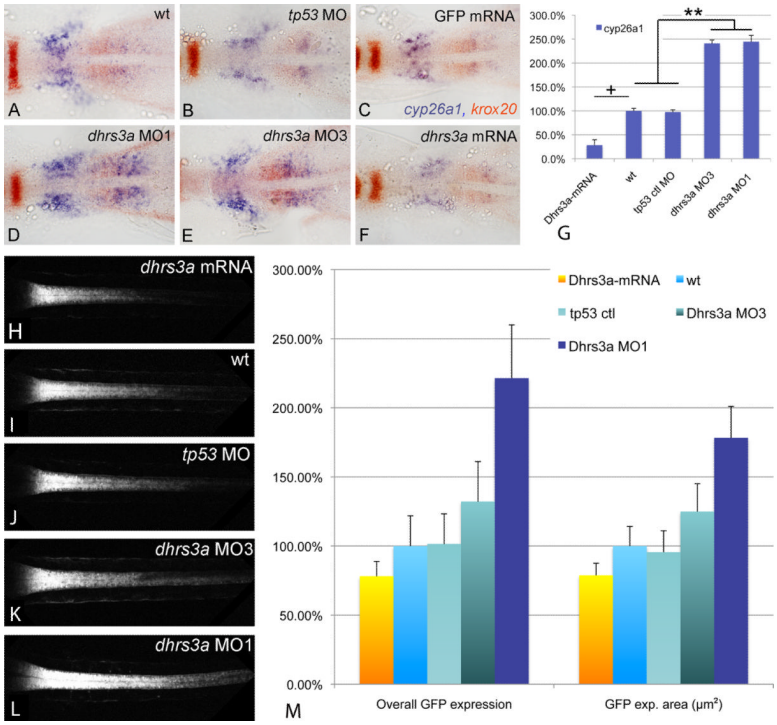

Figure 7. Dhrs3a functions as a regulator of RA signaling

(A-F) RNA *in situ* hybridizations on 5 somite stage embryos in dorsal view with anterior to the left, showing c*yp26a1* expression (blue) in the anterior trunk. Red staining is *erg2b* in rhombomere 5 and *aldh1a2* in the anterior paraxial mesoderm. (A) uninjected control embryo; (B) control embryo injected with 5ng *tp53MO*; (C) control embryo injected with 300pg GFP mRNA; (D) embryo injected with 5ng *dhrs3a* MO1 and 5ng *tp53* MO; (E) embryo injected with 5ng *dhrs3a* MO3 and 5ng *tp53* MO; (F) embryo injected with 300pg *dhrs3a* mRNA. (G) quantification of *cyp26a1* expression by qPCR. (H-L) projections of confocal images through the spinal cord of live *Tg(12XRARE-ef1a:gfp)sk71* transgenic embryos at 48hpf. The anterior limit of GFP expression corresponds to the rhombomere 6/7 boundary. ; (H) *dhrs3a* mRNA-injected embryo, (I) uninjected control, (J) control *tp53* MO-injected embryo; (K) *dhrs3a* MO3 plus *tp53* MO-injected embryo; (L) *dhrs3a* MO1 plus *tp53* MO-injected embryo. (M) quantification of live *Tg(12XRARE-ef1a:gfp)sk71* signal in n=6 injected with 300pg *dhrs3a* mRNA, n=6 uninjected, n=6 *tp53*MO (5ng/emb) injected, n=6 *tp53* + *dhrs3a* MO3 (5ng/emb each) injected and n=6 *tp53* + *dhrs3a* MO1 (5ng/emb each) injected embryos. “Overall GFP expression” is the sum of pixel intensities above background threshold; “GFP expression volume” is the total number of pixels in the confocal stack above background threshold. Values are normalized to the uninjected control.
** (ANOVA; The Newman-Kuels Test) $p<0.005$.
* (ANOVA; The Newman-Kuels Test) $p<0.05$. There is no significant difference on the GFP expression volume or overall signal between wt and *tp53*. + (Student T-test) $p<0.05$. *dhrs3a* mRNA injected embryos were normalized to control mRNA injected embryos.

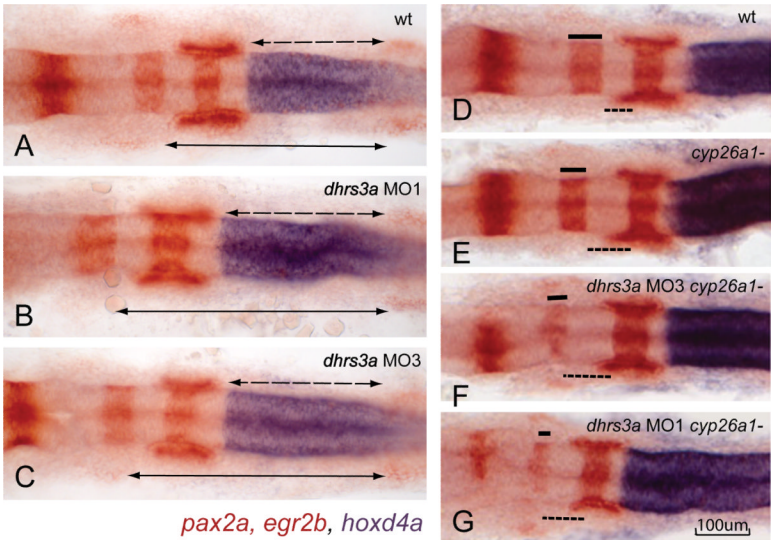

Fig 8. Dhrs3a knock-down effects nervous system patterning

(A-C), *in situ* hybridization of *hoxd4a* (blue), pax2a (red in mid-hindbrain boundary, otic vesicles and somites) and egr2b (red in rhombomere 3 and 5) in wt (A), *dhrs3a* MO1 (B) and MO3 (C)-injected embryos. Dotted arrows indicate the distance from the r6/7 boundary, marked by the anterior limit of *hoxd4a* expression, to the second somite (indicated by the anterior limit of *pax2a* expression). Solid arrows indicate the distance from the r3/4 boundary to the second somite. Both distances are longer in dhrs3a knock-down embryos. (DG) knock-down of Dhrs3 enhances the posteriorized hindbrain phenotype of *cyp26a1*$^{-}$ mutant embryos. (D) wt; (E); *cyp26a1-/gir* mutant; (F, G) *cyp26a1-/gir* mutant injected with *dhrs3a* MO3 (F) or MO1 (G).

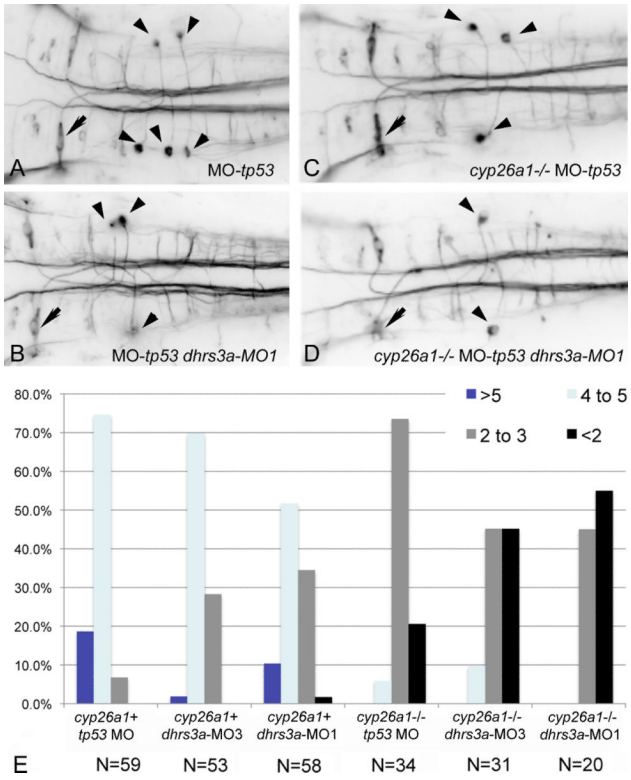

Figure 9. Dhrs3 knock-down effects hindbrain neuronal organization

(A-D) RMO44 immunostaining of hindbrain reticulospinal neurons. (A) control wt embryo with 5ng *tp53* MO; (B) *dhrs3a* MO1+*tp53* MO-injected embryo; (C) *cyp26a1* mutant embryo injected with 5ng control *tp53* MO; (D) *cyp26a1* mutant embryo injected with *dhrs3a* MO1+*tp53* MO. Arrows indicate the Mauthner neuron in r4, which is unaffected under all conditions; arrowheads indicate the distinctive T-interneurons which lie in r7 and anterior r8. (E) Quantification of the number of T-interneurons in each condition. N refers to the number of embryos counted.